Polarization-Insensitive and Angularly Stable Compact Ultrawide Stop-Band Frequency Selective Surface

Gouri Shankar Paul and Kaushik Mandal, *Senior Member, IEEE*

***Abstract*—In this letter, a compact ultrawide stop-band frequency selective surface (FSS) with polarization-insensitive and higher level of angular stability property is presented. It consists of a very simple modified square-ring unit cell that exhibits excellent wideband rejection over the entire ultrawideband (UWB) 2.72–13 GHz range. For TE incident wave, the <-20 dB bandwidth is 67.41% (5.01–10.1 GHz), which is 18.38% more compared to the simple square-ring-type FSS. This structure with the smallest unit cell dimension ($0.066\lambda_0 \times 0.066\lambda_0 \times 0.013\lambda_0$) compared to the earlier reported UWB FSSs is printed on a single-layer single-sided FR4 substrate. The design is flexible enough to tune the desired resonant frequency and the operating band by changing the length and width of the resonators. The design concept has been validated through proper measurement. This FSS can be used as a good reflector to enhance the gain of UWB antennas.**

***Index Terms*—Angular stability, frequency selective surface (FSS), polarization-insensitive, ultrawide stop-band.**

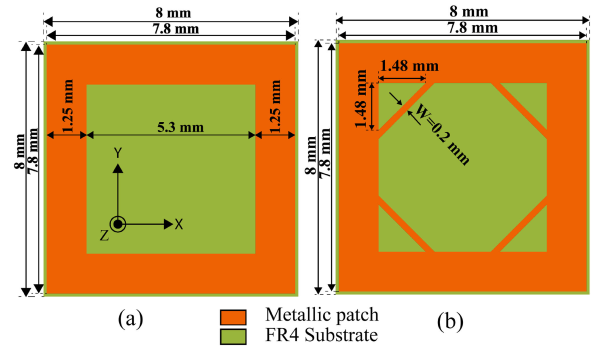

Fig. 1. Geometry of (a) simple square-ring FSS (Proposed 1) and (b) modified square-ring UWB FSS (Proposed 2).

I. Introduction

FREQUENCY selective surfaces (FSSs) have been investigated over the last few decades and drawn the major attention of many researchers for their numerous applications [1] such as radomes, spatial filters, absorber, radar cross section reduction, and many more. Recently, many researchers are working to develop the ultrawideband (UWB) (3.1–10.6 GHz) band-reject FSS for the performance enhancement of microstrip antennas.

Researchers adopted several techniques and structures like Dürer's pentagon-shaped prefractals unit cell [2], garland-like unit cell [3], and cross-dipoles-shaped [4] to design FSS with ultrawide stop-band characteristics. These wide band-stop FSSs are complex or consist of multiple layers and are unable to cover the entire UWB (3.1–10.6 GHz).

The reflective property of ultrawide stop-band multilayer FSSs [5]–[8] is successfully applied for the gain augmentation of microstrip antenna. When an antenna is placed at a finite distance above the FSS, the wave radiated towards the FSS is reflected. This adds to the direct outgoing wave radiated from the antenna in the opposite direction to the FSS reflector. The gain of the antenna in the presence of the FSS reflector will be maximum when two wave components are in phase, giving rise to constructive interference. Ranga *et al.* [5]–[7] did not show the angular stability and polarization-insensitive property of the proposed FSSs. The design [8] is angularly stable (up to 80°) but unable to exhibit the polarization-insensitive property due to its asymmetric unit cell structure.

Cross spiral patch and four H-shaped fractal parts-based FSS [9] shows higher incidence angle tolerances up to 75° over a narrow band (6.2–8 GHz). A dual-bandstop dual-layer FSS [10] consisting of incurving arms of conventional cross dipole exhibits a stable angular performance for incidence angles up to 60°.

Polarization-insensitive and angularly stable miniaturized but highly complex-type FSS [11] is printed on both sides of an ultrathin dielectric substrate for a single bandpass operation. Sivasamy *et al.* proposed a single-layer single-side ultrawide stop-band (4–14 GHz) FSS [12] with polarization-insensitive and angular-independent (up to 45° only) property. Recently, a similar type of UWB (4.5–14.7 GHz) FSS [13] is printed on the both sides of the substrate that exhibits angular-independent characteristic up to 60°. These UWB FSSs [12], [13] are highly polarization-insensitive with relatively lower level of incidence angle tolerances, and they fail to cover the lower cutoff frequency (3.1 GHz) of the UWB.

Therefore, there are some valid issues such as the size of the unit cell, the number of dielectric layers, angular stability, attenuation level, and accurately covering the entire UWB (3.1–10.6 GHz) that need to be considered during the design of the UWB FSSs with polarization-insensitive and angularly stable properties.

Manuscript received July 2, 2019; revised July 27, 2019 and August 3, 2019; accepted August 3, 2019. Date of publication August 7, 2019; date of current version September 4, 2019. *(Corresponding author: Kaushik Mandal.)*

G. S. Paul is with the Global Institute of Science and Technology, Indian Centre for Advancement of Research and Education Complex, Haldia 721657, India (e-mail: gourishankar.paul@gmail.com).

K. Mandal is with the Institute of Radio Physics and Electronics, University of Calcutta, Kolkata 700009, India (e-mail: kaushikrpe@ieee.org).

Digital Object Identifier 10.1109/LAWP.2019.2933545

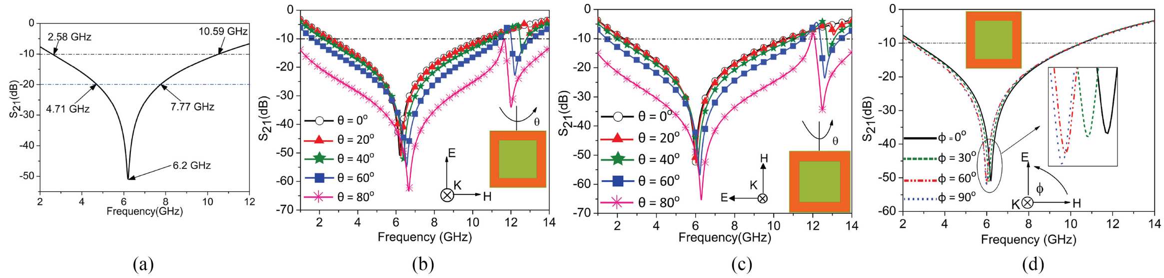

Fig. 2. Simple square-ring-type FSS. (a) Simulated S_{21} curve. (b) Simulated S_{21} curves for different incidence angles under TE polarization. (c) Simulated S_{21} curves for different incidence angles under TM polarization. (d) Comparison of S_{21} curves for different polarization angle under normal incidence.

Looking into the above issues, a very simple corner modified square loop patch-type FSS is designed using a single-layer single-side low-cost FR4 substrate with a unit cell dimension of $0.066\lambda_0 \times 0.066\lambda_0 \times 0.013\lambda_0$ (8 mm × 8 mm × 1.6 mm), where λ_0 corresponds to free-space wavelength at the lower cutoff frequency. This proposed modified square-ring FSS is polarization-insensitive with higher level of angular stability (≈80°), and attenuation level (47.8 dB), and is able to exhibit band rejection over 2.5–13.23 GHz, which sufficiently covers the entire UWB (3.1–10.6 GHz). Moreover, the unit cell of the proposed FSS is the simplest and smallest one in comparison to the earlier published related UWB FSSs. All the simulations are carried out using a finite element model (FEM)-based Ansys HFSS electromagnetic (EM) simulator.

II. Square-Ring-Type UWB FSS

From the analysis of a single square-loop FSS [14], one can design a band-reject FSS for a particular band. Similarly, a band-stop and a bandpass FSS can be designed using a square loop and slot structures [15], respectively. Initially, a simple square-ring-type FSS (Proposed 1), as shown in Fig. 1(a), is designed and analyzed. Next, a corner modified square ring patch is used to enhance the bandwidth of the stop-band. The proposed structure is designed on a single-side copper-cladded FR4 substrate of dimension $(8 \times 8 \times 1.6)\ \text{mm}^3$, $\varepsilon_r = 4.4$, and loss tangent of 0.02. A simple metallic square-ring-shaped patch with a 1.25 mm ring width is used to realize stop-band over the entire UWB.

The resonating wavelength is nearly equal to the circumference [1] of the square ring. If width of the ring is increased, then bandwidth can be increased. Therefore, by the proper adjustment of the square ring width and length, stop-band characteristic over the entire UWB can be achieved. Here, the proposed square-ring FSS exhibits bandstop over 2.58–10.59 GHz as shown in Fig. 2(a). The -10 and -20 dB fractional bandwidth is 121.64% and 49.03%, respectively. A good FSS should show stable response for different incidence angles, and it should be polarization-insensitive. Angular stability refers to a phenomenon in which the frequency response of the microwave structure remains unchanged by variation in the incidence angle of the incoming electromagnetic wave. The variation of S_{21} for different incidence angles for TE and TM polarization is shown in Fig. 2(b) and (c), respectively. It shows almost stable responses for 0° to 70° with a step of 20°. A little variation in center frequency has been observed for the incidence angle 60° and onwards, but as the desired stop-band is not affected, this little change can be neglected. The obtained results approved the expected higher angular stability characteristic of this FSS. Angular stability is generally observed for rotationally symmetric structures. A rotationally symmetric structure appears to be an anisotropic homogeneous medium for incident EM wave. The structure appears to be similar from whichever angle it is observed. The miniaturization of the structural unit improves the angular stability performance of the FSS as the phase variation is small over a structure whose dimensions are less. The proposed design is also polarization-insensitive as it shows nearly the same response for all polarization angles from 0° to 90° under the normal incidence wave, as shown in Fig. 2(d). This simple design is discussed for a better understanding of the final proposed FSS (corner modified square ring).

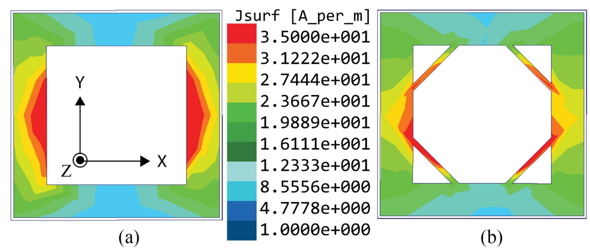

Fig. 3. Surface current distributions. (a) Simple square-ring unit cell. (b) Modified square-ring unit cell.

III. Modified Square-Ring UWB FSS

After analyzing the simple square-ring-type FSS, we observe that the <-20 dB stop-band bandwidth is nearly 3.06 GHz with relatively poor angular stability (≈70°). Now, to realize better reflectivity and angular stability, the four corners of the simple square-ring unit cell are modified without increasing the overall dimension of the unit cell (Proposed 2). Nearest arms of the square ring are connected by very narrow metallic strip of width 0.2 mm as shown in Fig. 1(b). This concept is conceived after analyzing the surface current distributions [see Fig. 3(a)] of a simple square-ring FSS. As the surface current is concentrated on the two side arms of the simple square-ring FSS, four narrow metallic strips are incorporated thinking that they will help to distribute the surface current and also reduce the path length. The above inference is confirmed through the surface current distributions [see Fig. 3(b)] on the proposed FSS structure at 7.39 GHz. As the path length decreases, the dip in transmission characteristic is shifted towards higher frequency and exhibits larger bandwidth. The transmission characteristic is shown in Fig. 4(a). This modified structure shows <-10 and <-20 dB stop-band over 2.5–13.23 and 5.12–9.74 GHz, respectively. Hence, the –10 and -20 dB fractional bandwidth is 136.42% and 62.18%, respectively. Thus, this proposed FSS provides 14.78% and 13.15% higher fractional bandwidth than the simple

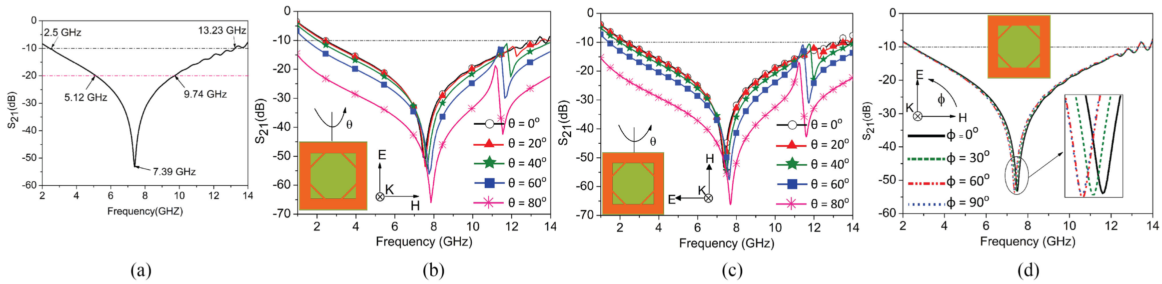

Fig. 4. Modified square-ring-type FSS. (a) Simulated S_{21} curve. (b) Simulated S_{21} curves for different incidence angles under TE polarization. (c) Simulated S_{21} curves for different incidence angles under TM polarization. (d) Comparison of S_{21} curves for different polarization angles under normal incidence.

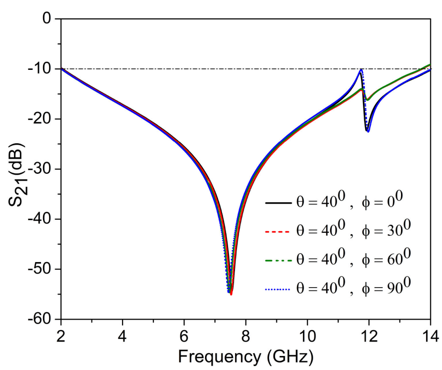

Fig. 5. S_{21} curves for different polarization angles under oblique incidence ($\theta = 40°$).

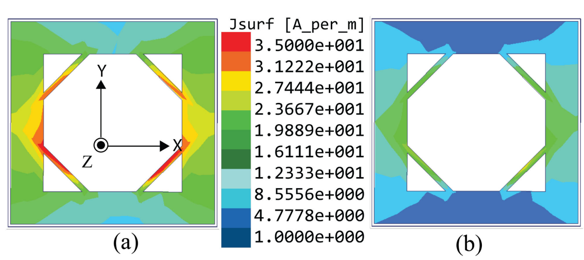

Fig. 6. Surface current distribution on the corner modified square-ring FSS. (a) 5.12 GHz. (b) 9.74 GHz.

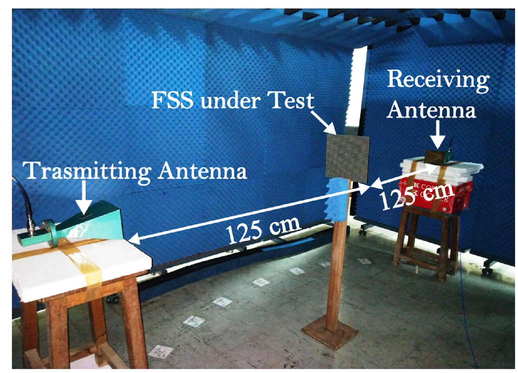

Fig. 7. Photograph of transmission coefficient measurement setup.

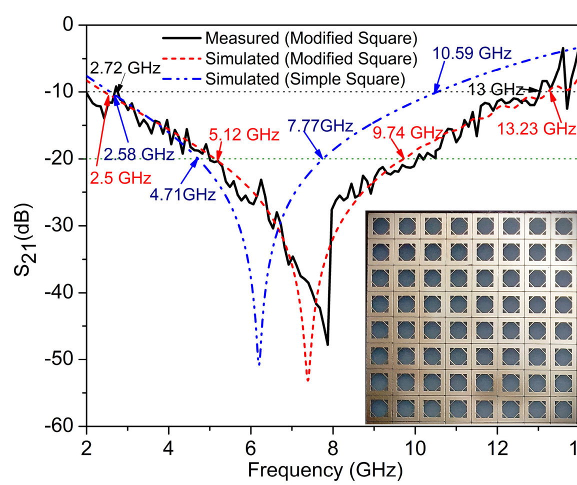

Fig. 8. Simulated and measured S_{21} curves for the proposed FSSs.

square-ring FSS for the –10 and −20 dB level, respectively. The angular stability under TE and TM polarization is shown in Fig. 4(b) and (c), respectively. For the incidence angle of 60° and 80°, the maximum deviation of the center frequency is only 0.3 and 0.4 GHz, respectively, whereas for the simple square-ring FSS, the deviation is 0.4 and 0.55 GHz, respectively. Hence, the proposed modified square-ring FSS exhibits better incidence angle tolerance due to symmetry in surface current distributions. Furthermore, the transmission characteristics for different polarization angles almost overlap with each other as shown in Fig. 4(d). To differentiate between Figs. 2(d) and 4(d), the area near the center frequency is zoomed for both figures and included in the inset of the corresponding figure. For the proposed 1 design [see Fig. 2(d)], it shows a larger deviation in comparison to the proposed 2 FSS. Therefore, the corner modified square-ring FSS is a better candidate in terms of polarization insensitivity also.

Under the oblique incidence ($\theta = 40°$) condition, changes in S_{21} characteristic due to the polarization angle (φ) variation are studied and shown in Fig. 5. It is observed that the overall bandwidth and the resonance frequency remain unchanged. This study fastens the polarization insensitivity of the corner modified square-ring FSS.

Considering the larger bandwidth of this structure, the current distributions at another two different frequencies (5.12 and 9.74 GHz) are studied as shown in Fig. 6 to analyze the stability of domain mode.

IV. Measured Results and Discussions

Both the structures (see Fig. 1) are proposed and analyzed for the first time. Only the corner modified square-ring FSS (Proposed 2) was fabricated and tested as it offers better performances in comparison to the simple square-ring FSS

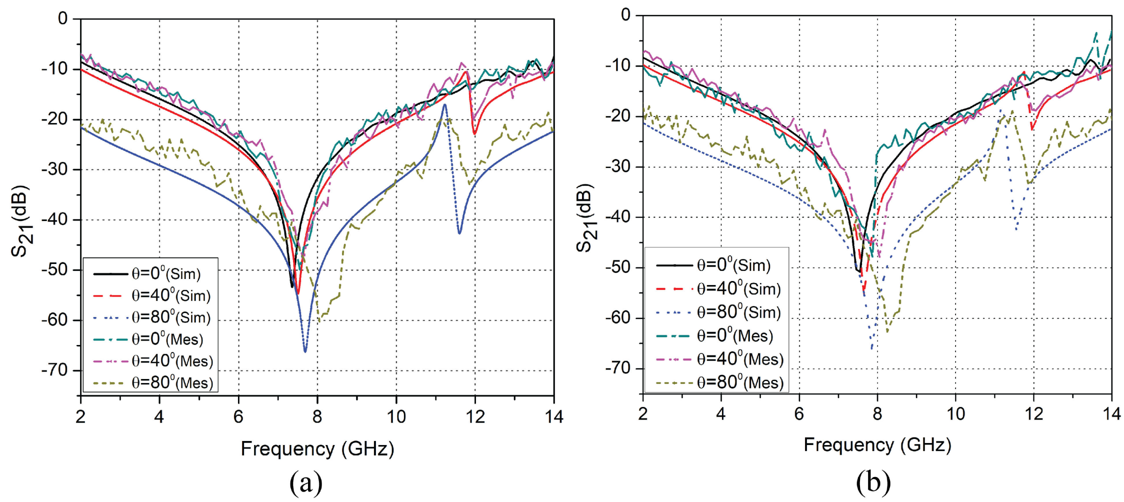

Fig. 9. Comparison of simulated and measured S_{21} curves for different incidence angle under (a) TE mode and (b) TM mode.

TABLE I
PERFORMANCE COMPARISON OF THE PROPOSED UWB FSS WITH THE PUBLISHED RELATED WORKS

Related works	Unit cell dimension (mm^3)	Operating band	-10 dB Fractional bandwidth (%)	-20 dB Fractional bandwidth (%)	Maximum attenuation level (dB)	Polarization insensitive	Angular stability
[6]	$0.09\lambda_0 \times 0.09\lambda_0 \times 0.007\lambda_0$ (single layer, single side)	3.5-10.6 GHz	100.7	42.3	67	No	-
[8]	$0.21\lambda_0 \times 0.21\lambda_0 \times 0.025\lambda_0$ (single layer, single side)	4.7-14.9 GHz	104.08	27	46	No	60°
[12]	$0.18\lambda_0 \times 0.18\lambda_0 \times 0.02\lambda_0$ (single layer, both side)	4-14 GHz	111.1	98.6	60	Yes	45°
[13]	$0.172\lambda_0 \times 0.172\lambda_0 \times 0.024\lambda_0$ (single layer, both side)	4.5-14.7 GHz	106.25	89.95	70	Yes	60°
Simple square ring FSS (Prop 1)	$0.068\lambda_0 \times 0.068\lambda_0 \times 0.0137\lambda_0$ (single layer, single side)	2.58-10.59 GHz	121.64	49.03	50	Yes	≈ 70°
Modified square ring FSS (Prop 2)	$0.066\lambda_0 \times 0.066\lambda_0 \times 0.013\lambda_0$ (single layer, single side)	2.72 –13 GHz	130.78	67.41	47.8	Yes	80°

(Proposed 1). The dimension of the fabricated FSS is 256 × 256 mm^2, which contains 32 × 32 elements. A transmission coefficient measurement setup is shown in Fig. 7. The measured transmission coefficient shows a good agreement with the simulated one, as shown in Fig. 8. The photograph of the fabricated prototype is shown in the inset of Fig. 8. The measured transmission characteristic shows <-10 and <-20 dB stop-band over 2.72–13 GHz (130.78%) and 5.01–10.1 GHz (67.41%), respectively, with a maximum attenuation level of 47.8 dB, which ensure the good reflectivity feature of this FSS. The -20 dB fractional bandwidth of the modified square-ring structure is 18.38% more in comparison to the simple square-ring FSS.

The simulated and measured S_{21} curves for different incidence angle under TE and TM polarizations are shown in Fig. 9. Due to the fabrication tolerances and measurement environment, the measured S_{21} curves slightly deviated from the simulated one. To show the novelty, advantages, and compactness of the proposed FSS over the related design proposed by different researchers, a comparative study has been carried out and summarized in Table I. The comparison is done based on a unit cell size, an operating band, –10 dB fractional bandwidth, a maximum attenuation level, polarization insensitivity, and a degree of angular stability. According to the table, the proposed FSS is able to cover maximum bandwidth with miniaturized dimension, good angular stability, and also polarization insensitivity using only a single-layer single-side simple FSS. The proposed FSS is 61.62%, 26.66%, and 2.94% compact in comparison to the most related works [13], [6], and the simple square-ring FSS, respectively.

V. CONCLUSION

A very simple and most compact ultrawide stop-band FSS has been presented and studied thoroughly to validate its polarization-insensitive and angular stability performances. A simple square-ring patch has been conceived and modified by adding four corner strips to enhance the -20 dB impedance bandwidth and attenuation level for the better reflectivity performance and incidence angle tolerance. In comparison to the related published works, this design is able to exhibit better angular stability, polarization insensitivity, and band rejection over the entire UWB.

ACKNOWLEDGMENT

The authors would like to thank Prof. P. P. Sarkar, Department of Engineering and Technological Studies, University of Kalyani, and Dr. S. Bhattacharyya of the Indian Institute of Technology (Banaras Hindu University), Varanasi, India for providing their measurement facilities. The authors would also like to thank the reviewers and the Associate Editor for their useful comments in improving this manuscript.

REFERENCES

[1] B. A. Munk, *Frequency Selective Surfaces: Theory and Design*. New York, NY, USA: Wiley, 2000.

[2] J. I. A. Trindade, P. H. F. Silva, A. L. P. S. Campos, and A. G. D. Assunção, “Analysis of stop-band frequency selective surfaces with Dürer’s pentagon pre-fractals patch elements,” *IEEE Trans Magn.*, vol. 47, no. 5, pp. 1518–1521, May 2011.

[3] S. Baisakhiya, R. Sivasamy, M. Kanagasabai, and S. Periaswamy, “Novel compact UWB frequency selective surface for angular and polarization independent operation,” *Prog. Electromagn. Res. Lett.*, vol. 40, pp. 71–79, 2013.

[4] I. S. Syed, Y. Ranga, L. Matekovits, K. P. Esselle, and S. G. Hay, “A single-layer frequency-selective surface for ultrawideband electromagnetic shielding,” *IEEE Trans. Electromagn. Compat.*, vol. 56, no. 6, pp. 1404–1411, Dec. 2014.

[5] Y. Ranga, L. Matekovits, K. P. Esselle, and A. R. Weily, “Multioctave frequency selective surface reflector for ultrawideband antennas,” *IEEE Antennas Wireless Propag. Lett.*, vol. 10, pp. 219–222, 2011.

[6] R. Yahya, A. Nakamura, and M. Itami, “Low profile UWB frequency selective surface based antenna,” *ITE Trans. MTA*, vol. 4, pp. 369–374, 2016.

[7] S. Kundu, “Gain augmentation of a CPW fed printed miniature UWB antenna using frequency selective surface,” *Microw. Opt. Technol. Lett.*, vol. 60, pp. 1820–1826, 2018.

[8] P. Das and K. Mandal, “Modeling of ultra-wide stop-band frequency selective surface to enhance the gain of a UWB antenna,” *Microw., Antennas Propag.*, vol. 13, pp. 269–277, Feb. 2019.

[9] Z. Zhao, H. Shi, J. Guo, W. Li, and A. Zhang, “A stop band frequency selective surface with ultralarge angle of incidence,” *IEEE Antennas Wireless Propag. Lett.*, vol. 16, pp. 553–556, 2017.

[10] A. Kocakaya and G. Çakır, “Novel angular-independent higher order band-stop frequency selective surface for X band,” *Microw., Antennas Propag.*, vol. 12, pp. 15–22, 2017.

[11] A. B. Varuna, S. Ghosh, and K. V. Srivastava, “An ultrathin polarization insensitive and angularly stable miniaturized frequency selective surface,” *Microw. Opt. Technol. Lett.*, vol. 58, pp. 2713–2717, 2016.

[12] R. Sivasamy, B. Moorthy, M. Kanagasabai, J. V. George, L. Lawrance, and D. B. Rajendran, “Polarization-independent single-layer ultra-wideband frequency-selective surface,” *Int. J. Microw. Wireless Technol.*, vol. 9, pp. 93–97, 2017.

[13] D. Sood and C. C. Tripathi, “Polarization insensitive compact wide stop-band frequency selective surface,” *J. Microw. Optoelect. Electromagn. Appl.*, vol. 17, pp. 53–64, 2018.

[14] K. R. Jha, G. Singh, and R. Jyoti, “A simple synthesis technique of single-square-loop frequency selective surface,” *Prog. Electromag. Res. B*, vol. 45, pp. 165–185, 2012.

[15] D. Ferreira, R. F. S. Caldeirinha, I. Cuiñas, and T. R. Fernandes, “Square loop and slot frequency selective surfaces study for equivalent circuit model optimization,” *IEEE Trans. Antennas Propag.*, vol. 63, no. 9, pp. 3947–3955, Sep. 2015.